Mini Mechanically Pumped Loop Modelling, Design and Tests for standardized CubeSat thermal control

J. van Es[1] , T.V. Ganzeboom.[2], T.H. van den Berg[3] and A. van Vliet[4]
Netherlands Aerospace Centre, Marknesse, The Netherlands

H.S.B. Brouwer[5]
ISIS – Innovative Solutions In Space, Delft, TheNetherlands
and

S. Elvik[6]
DEMCON, Enschede, The Netherlands

With the miniaturization of space-borne sensors and introduction of small propulsion modules, more powerful payloads are anticipated to be used in small satellites. Therefore, new thermal concepts are required to cope with the increasing thermal dissipation and the negative effects. This paper presents a new thermal control concept to thermally standardize small satellites with power dissipation problems and making them thermally independent of their orbits.

This new thermal design concept is a mini Mechanically Pumped Loop (MPL). The design of the mini-MPL takes into account the requirements imposed by CubeSats and their subsystems, thereby ensuring its compatibility with small satellites and a variety of missions. The heart of the system is the multi-parallel micro-pump (MPMP) as developed by the Netherlands Aerospace Centre (NLR). This pump concept provides a low mass MPL solution with high reliability. Subsequently, the article describes the concept of the loop and pump and micro-pump test results are presented. The Mini-MPL is also modelled in Matlab to support MPL system design trade-offs. The model is described and modelling results are presented and included in the elaborate working fluid selection given. Finally, the advantages and drawbacks of the system are elucidated by comparison with conventional thermal design options. The paper concludes with an outlook on further development and mini-MPL applications.

Nomenclature

ρ	=	Fluid density (kg/m^3)
μ	=	Dynamic viscosity (N/m^2 s or kg/(ms))
c_p	=	Specific heat capacity (J/(kg K))
d	=	Inner diameter tube (m)
L	=	Tubing length in the mini-MPL (m)
$\dot{m}$	=	Mass flow (kg/s)
T	=	Temperature (K)
P	=	Power (W)
p	=	pressure (N/m^2)
MLI	=	Multi Layer Insulation
P/L	=	Payload
(L)HP	=	(Loop) Heat pipe
PCM	=	Phase Change Material
MPMP	=	Multi Parallel Micro Pump
MPL	=	Mechanically Pumped Loop
TRL	=	Technology Readiness Level

[1] *Principal Scientist, Thermal Control Group Aerospace Division, Johannes.van.es@nlr.nl*
[2] *Thermal Engineer, Thermal Control Group Aerospace Division, Thomas.ganzeboom@nlr.nl*
[3] *Thermal Engineer, Thermal Control Group Aerospace Division, Ramon.van.den.berg@nlr.*
[4] *Application Engineer, Thermal Control Group Aerospace Division, Adry.van.vliet@nlr.nl*
[5] *Systems Engineer, ISIS - Innovative Solutions In Space BV, h.brouwer@isispace.nl*
[6] *Sr. Mechatronic System Engineer, DEMCON, Sander.elvik@demcon.nl*

I. Introduction

With the introduction of commercial swarms of satellites, standardisation of satellite subsystems and components becomes a critical requirement for success. To get an idea the of the power available on Cubesats, the power versus mass trend is shown in Figure 1.

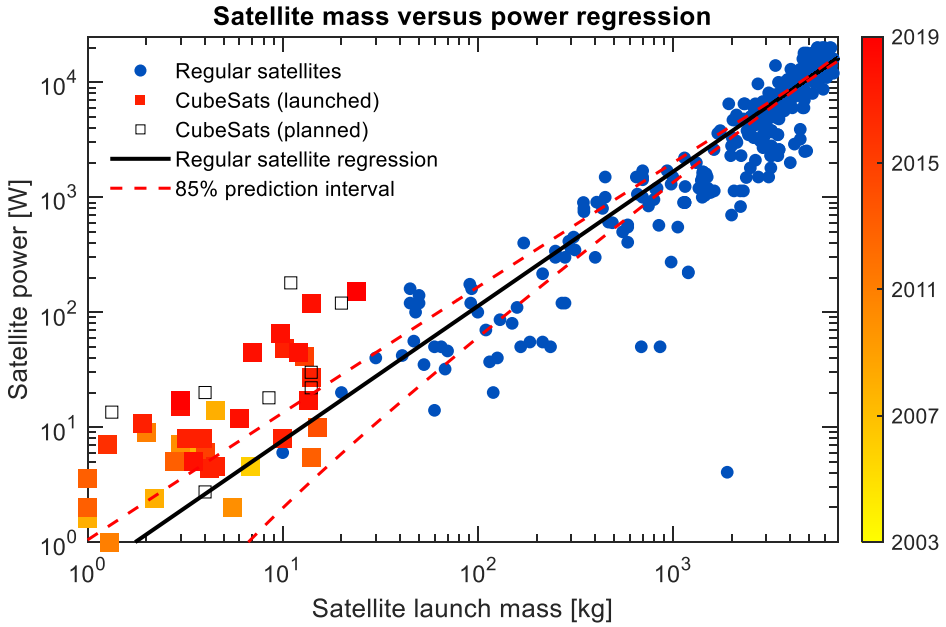

Figure 1: Mass versus power trend line for satellites (modified by including data of state-of-the-art CubeSats 1U – 16U) including a color gradient for the CubeSat datapoints for older (yellow) and newer (red) CubeSats [1].

With the increasing power of Cubesats, thermal subsystems become also relevant for standardization. Thermal problems will only occur for Cubesats with a significant amount of power. It is assumed that above 20 Watts the Cubesats can experience thermal problems which require an active Thermal Control System (TCS). Translated into the satellite classifications this means that until the size of pico-satellites a thermal concept is obsolete. A general thermal concept starts to be interesting for microsatellites and the high-end of nanosatellites with additional deployable solar panels as summarized in Table 1. Main conclusion is that an active Thermal Control System (TCS) becomes relevant for satellites of 3U CubeSat size with large deployable solar panels or 8U without deployable solar panels. The thermal concept described below is therefore focused for CubeSats of 6U and larger [2].

At present, there is no active Thermal Control System (TCS) available for Cubesats and small sats (<100 kg), and thermal issues are resolved using passive means (radiation and to some extent heat pipes). However, as these satellites evolve, grow in size and/or become more capable, these passive means of thermal control no longer suffice, and an advanced TCS is required. In itself, such a TCS is also an enabler of new missions and capabilities, meeting the market trend:

Table 1: Small satellite classifications and severity of thermal design challenges

Satellite Classification	Mass range	CubeSat size	Potential severity of thermal challenges	Remarks
Femto-satellite	(0.01–0.1 kg)			No power to create thermal problems
Pico-satellite	(0.1–1 kg)			No power to create thermal problems
Nano-satellite	(1–10 kg)	1U-8U		
Micro-satellite	(10–100 kg)	>8U		
Mini-satellite	(100–500 kg)			

- Larger Cubesats (> 12 U / 10 kg):
    - in particular for communication or propulsion modules (having high heat generation);
    - with unfavorable distribution of heat source and sink
- The advent of deployable solar arrays on CubeSats, increasing their possible power consumption

More specific, it is expected [3] that Advanced Thermal Control Systems (TCS) for CubeSats are already relevant for missions which have:

a) Electric propulsion;
b) High power RF payloads, such as radars;
c) High power transceivers for communication with Earth or inter-satellite links
d) Interplanetary missions with tight power constraints, where heat switching capabilities will reduce the heater requirement.

II. Requirements for a standardized thermal control system for CubeSats

Prior to the development of a standardized thermal concept a list of requirements was determined. The key requirements for a CubeSat TCS are listed here:

- Low cost
- Low volume (fit in 1U)
- Low power consumption (<3 Watt in all orbital cases)
- Heat removal capability of 20-100W
- Heat switch capability to minimize heater power during eclipses
- Modular and flexible to integrate in CubeSats
- Flexible to connect to payload (P/L) dissipative elements

As for all subsystems, the TCS needs to be low cost, small in volume, have low power consumption and must be modular and flexible to integrate in CubeSats.

An additional requirement which is important for CubeSats is the heat switch function. When a satellite enters eclipse, the temperature of the radiator decreases rapidly and without a heat switch the temperature of the P/L will decrease as well. To mitigate this problem, a heater with equal power input as the P/L, is typically placed on the P/L to keep the P/L temperature within survivable range. This adds an additional power draw on the batteries during every eclipse. To combat this issue, radiators are typically down-sized which results in less over-cooling during eclipse, allowing for a smaller heater, but this also reduces the operational window of the P/L. With more and more demanding P/L´s this is one of the major issues to be solved by a standardized thermal solution for small spacecraft. Apart from a direct advantage for the P/L operational window, a heat switch function also gives more flexibility and increases the survivability during survival modes and unwanted tumbling of small satellites.

III. Mini-Mechanically Pumped Loop concept

The technology presented here is an advanced thermal control system providing the following performance/functionality:

- Heat removal capability: at least 20 W and scalable up to 200 W;
- CubeSat standards compatible, stowed volume less than 1U;
- Heat switch function by switching off the pump in cold conditions to reduce heater power in eclipses;
- Flexibility in platform thermal design and component distribution, is able to service multiple hot spots;
- Flexible tubing allowing for mechanical decoupling of P/L and frame, reducing the stresses on PCB components during launch

The base of the technology is the Multi-Parallel Micro-Pumped one-phase Loop (MPMPL) developed at NLR. This technology is currently at TRL 3.

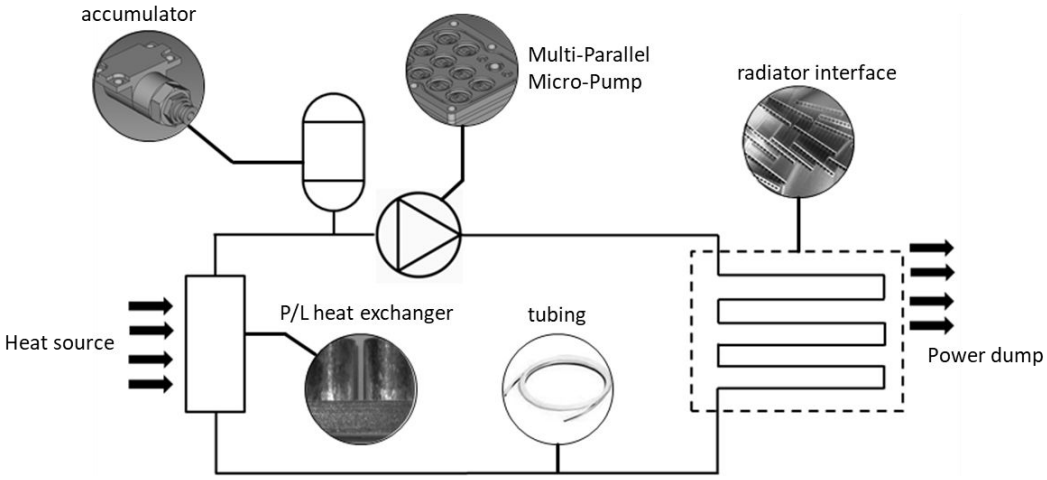

Figure 2: Mini-MPL Schematic

The mini-MPL transports dissipated heat from hot spots to thermal radiators. The loop is shown in Figure 2. The liquid is transported by the pump to a heat exchanger mounted on a thermal hot spot, where the liquid collects the heat and cools the hot spot. The liquid flows back via the thermal radiators where the heat is radiated into deep space. The hot spot interface is connected with small diameter flexible tubing and is suitable to be routed along multiple and/or different types of hot spots. An accumulator allows for thermal expansion/contraction of the working liquid due to the large temperature fluctuations in space. The pump and accumulator in a typical MPL are placed on the 'cold' side of the loop, after the radiator. In this case the pump and accumulator are placed after the P/L on the 'hot' side of the loop. This is advantageous as the accumulator operates at an elevated temperature compared to the rest of the loop (see section V.B) and the conductive heat loss is minimized if the accumulator is placed on the warmer side of the loop.

IV. MPL comparison with conventional thermal solutions

The Mini-MPL is not the only thermal solution which can address the CubeSat thermal challenges. Also heat pipes (HPs), mini LHP's, Phase Change Materials (PCM) and thermal straps are potential solutions. The main advantages and drawbacks of these systems compared to the mini-MPL are given in Table 2. It follows that the main advantages of a mini-MPL are the flexibility and the modularity. The main drawback is the active nature of the mini-MPL. The reliability problem is however addressed well by the multi-parallel-micro-pump concept. For CubeSat thermal subsystem design, flexibility is of key importance to allow for a quick response to market demands of swarm customers.

Table 2: Comparison between mini-MPL and alternative thermal control solutions for CubeSats

Thermal solution	Comparison with mini-MPL	
	Advantages	**Drawbacks**
HP's	Simple, low cost, well-known, No active components	Inflexible and non-modular design Limited amount of hot spots can be addressed Rigid connection between PCB connection and CubeSat frame Low reliability of heat switch function
Mini-LHP's	No active components, well-known	Inflexible and non-modular design Limited amount of hot spots can be addressed No or heavy heat switch capability
PCM	No active components, low-cost, well-known,	Inflexible for late orbital changes Limited amount of hot spots can be addressed
Thermal straps	No active components, reliable, low cost	Low thermal performance No heat switch capability

The short development time implies there is no longer time for extensive thermal analyses to verify whether the swarm satellites survive the worst case conditions of all orbits involved. This makes passive thermal control solutions less attractive as they require a full set of thermal analyses. Therefore thermal designs with (simple) active control become beneficial as they allow the thermal S/C designer to take control in extreme conditions.

V. MPL prototype design

A. Multi-Parallel Micro-pump

The heart of the mini-MPL is a multi-parallel-micro-pump and creates flow by 10-30 pumps in parallel. This design avoids the single-point of failure of a pumped loop. If one pump fails, still *n-1* pumps are left to provide flow, which drops relatively to *(n-1)/n* fraction of the original flow.

The single micro-pumps used as building blocks, are piezo-driven displacement pumps with passive micro-valves (Figure 3 right). The design is made specifically to fit with the CubeSat modular set-up with mainly PCB's. This has the additional advantage of lower static pressure differences between pump and therefore a performance which is more equivalent with micro-g operations. The demonstration pump (Figure 3 left) has 5 parallel micropumps per plate (Figure 3 middle), each micropump consisting of 2 piezo pumps in series. The design is completely modular and more plates with piezo pumps can be added for increased flow. The pump housing is stacked using bolts and sealed with rubber O-rings. Future pumps will be metal printed in titanium and will be hermetically sealed from the outside by laser welding. The unoptimized stainless steel prototype pump has a total weight of 0.6 kg. Using titanium instead of stainless steel, welds instead of bolts, and general optimizations to the design, it is expected that future pumps have a total mass below 0.3 kg.

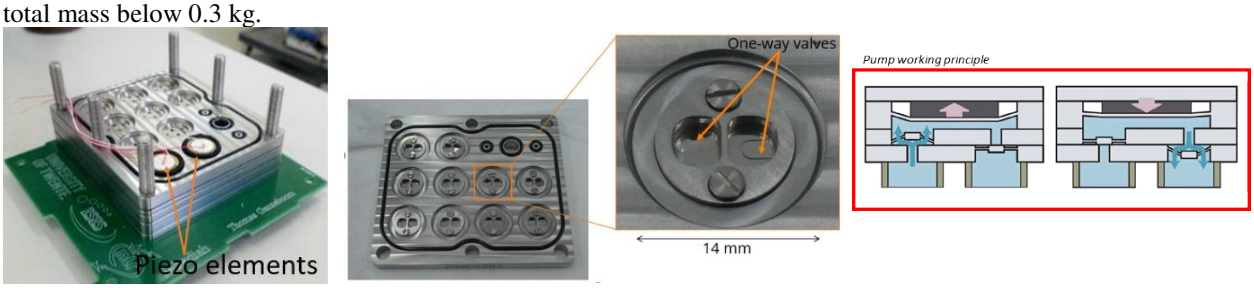

Figure 3: Multi-parallel-micro-pump, left: MPMP pump stack, middle: Single pump plate with single piezo pump enlarged, right: Operational principle of a single piezo chamber.

The valve design has been investigated and optimised with regards to previous iterations to improve the MPMP robustness and performance. A typical measured pump curve for a single micro-pump with a 10 µm valve is given in Figure 4.

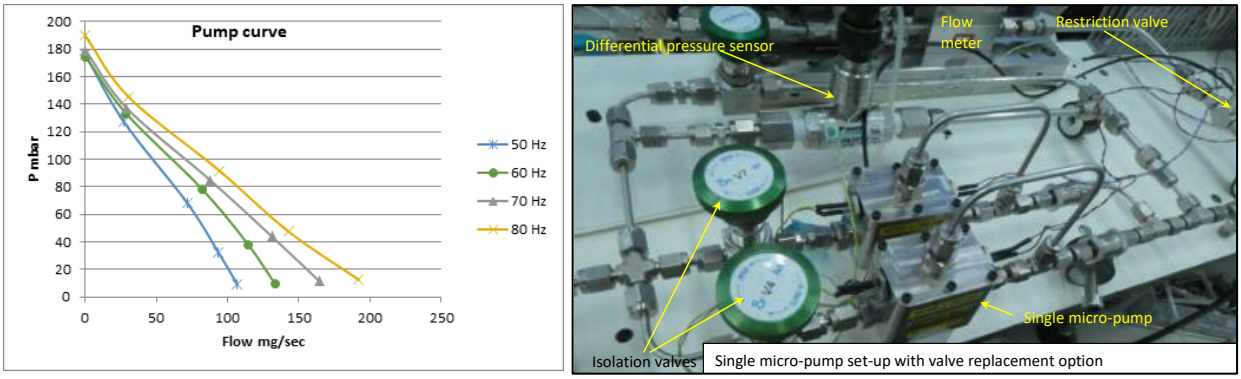

Figure 4: Left: Micro-pump curve for a 10 µm thick valve with several piezo frequencies, Right: Test set-up

B. Accumulator

Although the mini-MPL is a single-phase loop, the accumulator used is a two-phase accumulator. The system pressure is maintained by keeping the accumulator above a defined saturation temperature. This concept is more robust for

launch vibrations and it allows for future upgrades to mini two-phase MPL's with much larger heat removal capabilities. The accumulator exists of a stainless steel container with an attached heater to keep the accumulator temperature above a threshold value. A porous filter is used for vapour blocking and liquid transport to the heater location.

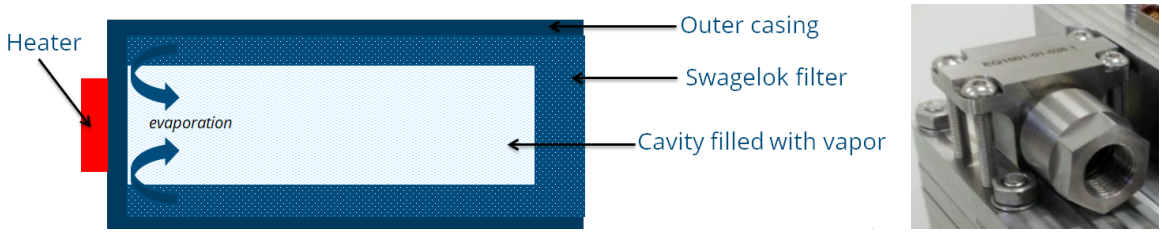

Figure 5: Left: Two-phase accumulator design; Right: Picture (Volume is 2.5 mL)

C. Other loop components

The MPL further contains a payload heat exchanger which can be glued to hot spot components on PCB's in the CubeSat. Either procured parts or 3D printed Aluminum is foreseen. The mini-MPL electronics are limited to the MPMP Electronics of which a prototype is already made which uses Commercially avaialable Off-The-Shelve (COTS) electronics. The radiator interface selected is a multi-port extruded aluminum strip which can be connected to the outside of the CubeSat or a dedicated radiator. This reduces the ΔT on the radiator side to the minimum possible. The tubing used is made of fluoropolymer (PFA), which is a flexible material with a low thermal conductivity. This allows the tubing to mechanically decouple the PCB hot spot and the CubeSat frame. The low thermal conductivity is beneficial to the heat switching functionality of the MPL system.

D. Mini-MPL single phase modelling

In order to analyze the mini-MPL's thermal performance the available NLR two-phase MPL software [4] is adapted for single-phase operation and to the smaller size of mini-MPL's. A typical model result is shown in Figure 6. This model is used in sizing the loop components as well as performing the fluid trade-off described in the next section.

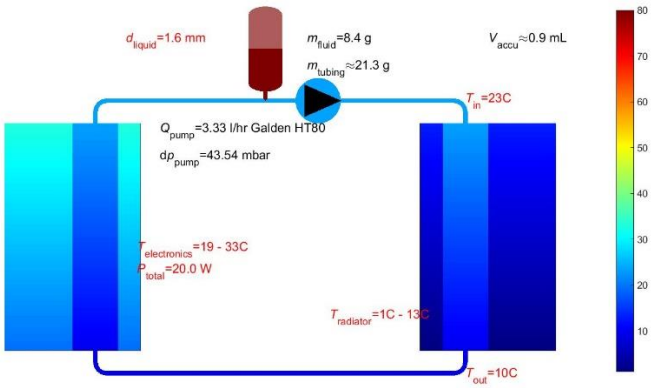

Figure 6: Single-phase mini-MPL model result with Galden HT80

VI. Mini-MPL working fluid

A working fluid is selected to fulfil the requirements of the preliminary system. First a pre-selection of working fluids from all possible coolants is made. This is done using the figure of merit method [5] for single phase mechanically pumped fluid loops. The figure of merit method ranks potentially interesting working fluids based on the following criteria (merits).

- **Minimal pressure drop in the system**, denoted as M_{pump}
- **Minimal required pump power**, denoted as M_p
- **Minimal size of the accumulator**, denoted as M_{acc}

The first two figures of merit are based on the pressure drop, the last on the thermal expansion of the fluid. The working fluid dependent properties on pressure drop are therefore isolated from the geometry dependent properties [5].

$$\Delta p \propto \overbrace{\left(\frac{\mu_l^{1/4}}{\rho_l Cp^{7/4}}\right)}^{\text{fluid dependent}} \overbrace{\frac{L}{d^{19/4}} \frac{P^{7/4}}{\Delta T^{7/4}}}^{\text{geometry dependent}} \quad \text{Heat input and sensible temperature difference of the fluid} \tag{1}$$

Pressure head figure of merit

The working fluid figure of merit for pressure head is then given by the inverse of the fluid dependent pressure drop term. An example result graph is shown below. Minimizing the potential pressure drop in the system is an important aspect in MPL design, as it determines the maximum length and minimum diameter of the tubing.

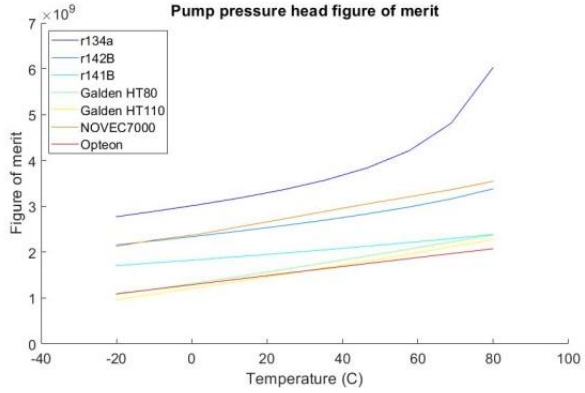

$$M_{\Delta p} = \frac{1}{\mu_l^{1/4} / (\rho_l c_p^{7/4})} \tag{2}$$

Pump power requirement figure of merit

As power supply is limited on board any spacecraft, and especially CubeSats, it is important to take into account the power consumption of the pump in the mini-MPL. The figure is based on the product of the pressure drop and the volume flow required which is proportional with density and sensible heat.

$$M_{pump} = \frac{\rho_l c_p}{\mu_l^{1/4} / (\rho_l c_p^{7/4})} \tag{3}$$

As one of the requirements for the MPL design is minimal power consumption, it is useful to select a working fluid that requires the least amount of power to transfer a certain amount of heat.

Accumulator size figure of merit

The third figure of merit is related to the accumulator in the MPL. It is beneficial for both volume and mass to have an accumulator that is as small as possible. The accumulator size is proportional to the expansion of the work fluid at minimum and the maximum operational temperature. The working fluid dependent part is present in the below figure of Merit.

$$M_{\text{acc}} = \frac{\rho_{Tmax}}{\rho_{Tmin} - \rho_{Tmax}} \tag{4}$$

The available volume for the MPL design on-board a CubeSat is very limited. Therefore it is important to choose a working fluid with a small thermal expansion coefficient so that the accumulator can be as small as possible.

Each investigated fluid scores points on each of the aforementioned merits. The coolant r134a is used as a baseline and all scores are normalized with respect to the score of r134a. The higher the score, the better the working fluid is suited for this specific criterium. If a score is above 1, it means that this working fluid outperforms r134a in a typical single phase MPL application. This analysis results in a short-list of potentially interesting working fluids. An

overview of the short-list of fluids with their respective scores can be seen in Table 3. For the analysis an operating temperature range of -20°C to +80°C was used.

Based on the result of the figure of merit analysis it can be stated that the most promising candiates are Opteon SF10, Galden HT110 and Galden HT80.

Table 3: Figure of merit results of selected working fluids compared to r134a which is used as a baseline.

Fluid name	M_{pump}	M_p	M_{acc}	Average
R134a	1	1	1	1
R142B	0.78	0.65	1.64	1.02
NOVEC 7000	0.77	0.78	1.99	1.18
R141B	0.62	0.51	2.61	1.25
Galden HT80	0.39	0.33	3.65	1.46
Galden HT110	0.42	0.40	3.70	1.51
Opteon SF10	0.39	0.35	4.36	1.70

To arrive at a final fluid choice a detailed analysis is done by performing full system calculations on a simplified MPL loop. The analysis is performed for each of the pre-selected working fluids. The following aspects are included in the analysis:

- Maximum tube length with given pump head
- Required pump power
- ΔT at the nominal heat load
- Accumulator volume
- Operating pressure
- Heat transfer coefficient (ΔT from tube to wall)

The calculations are performed with the following assumptions:

- **Pump performance**
  A single NLR micro-pump has a capacity of 200 mg/s and a maximum pressure head of 100mbar. Ten pumps in parallel are assumed with a total flow of 2 g/s and pressure head of 100 mbar. A conservative pump efficiency of 5% is assumed
- **Heat removal capacity**
  The required heat removal capacity is set to 100 W.
- **Radiator environment and properties**
  A deep space temperature of 4 Kelvin is assumed. Additionally the temperature of the surface of the earth is estimated to be around 10° C. The radiators on the CubeSat are assumed to have an emissivity coefficient of 0.9. The heat absorbed from the sun is not taken into account.
- **Tubing**
  A tubing diameter of 3 mm is assumed.

The results as presented in Table 4 are colour coded; dark green indicates it is the best result and light green indicates the second best. The colour orange indicates a possibly problematic result which could exclude the fluid from further evaluation.

All tube lengths are acceptable and therefore the pressure head is not a design driver. For the pump power the Galden fluids perform the best due to the large density and sensible heat values. The difference is however not large enough to discriminate between liquids. The ΔT which is related to both sensible heat and the heat transfer coefficient is a measure for how much heat can be collected before the maximum payload temperature is reached. R134a is performing best and the worst alternatives have a 15° C additional temperature rise. For small systems this value is not yet driving but for extensions in the future a low ΔT is preferred. As the system operates with a two-phase accumulator to pressurize the system the required saturation temperature for a 1.5 bar operating is presented. Preferred

liquids have a saturation temperature above 20 °C but not exceeding 100 ° C. This excludes Galden HT110 and Opteon SF10.

Another real system driver is the operating pressure at 80 °C, this is the system pressure expected during operation. Pressures above 10 bars are excluded because of impact on mass and design flexibility. On the other hand pressures below 1 bar are also problematic during testing. Any leak results in air and water vapour in the system with potential detrimental effects on pump operation and fluid characteristic in case of a hygroscopic fluid. The goal then is to obtain an operating pressure that is only slightly above 1 bar to minimize the impact of high pressures on the design. This is most easily achieved when using Galden HT80 or by using NOVEC 7000. For R134a and R142b the pressures are too high to be acceptable.

The main mass driver is the accumulator size. Opteon performs here best with Galden and Novec liquids as second best. Here R134a underperforms significantly which is the main reason R134a is not favourable for space applications.

The last aspect listed is the heat transfer coefficient. With the low power densities in CubeSats and the various new technologies of increasing heat transfer area at low cost by e.g. metal printing this aspect is less important than in larger TCS. Here R134a is outperforming all other fluids.

Based on the above results Galden HT80 is selected as preferred working fluid and used in the detailed design phase as baseline. During testing, Galden HT55 is used as working fluid, due to limited availability of Galden HT80.

Table 4: Cooling loop parameters for selected work fluids at 100W heat load without pre-heater with Tset=20°C.

	Max. L_{tube}	Req. Pump power	ΔT of the liquid at 100W	T_{sat} at 1.5 bar	Operating pressure at 80 °C	V_{acc}/V_{loop}	Heat transfer
Fluid name	m	W	°C	°C	Bar	%	W/m²K
R142B	20	0.35	39	2	13.8	8.6	236
R141B	19	0.32	44	44	4.2	6.7	190
R134A	23	0.32	36	-16	26.3	10.9	260
Galden HT80	20	0.24	52	97	0.94	6.1	102
Galden HT110	18	0.23	48	123	0.33	5.5	90
NOVEC 7000	21	0.28	39	48	4.1	7.8	172
Opteon SF10	17	0.25	50	124	0.35	5.0	95

VII. Prototype testing

From the MPL design a prototype was constructed to serve as a proof of concept and to validate the numerical model. The pump and accumulator are tested separately to determine their performace.

A. Pump testing

The pump was placed in a test-setup of which the schematic can be seen in Figure 7 on the left. The pump was outfitted with 5 parallel micropumps, each containing 2 piezo pumps in series. All pump tests were performed under slightly elevated pressure (~1.3 bara).

A system curve of the test setup was determined by applying a mass flow using an external pump while measuring the pressure drop of the overall system. This measurement includes the micropump stack that will be tested, so the pressure drop in the pump housing is also known. Next, the pump curves of each of the 5 parallel micropumps are determined separately. This is done by switching on a single micro pump in the pump stack consisiting of two piezo elements in series. A flow restriction is applied and gradually increased to determine the pump performance at a specific input voltage and frequency. The results can be seen in Figure 7 on the right, where it can be seen that not all pumps perform equally. Pump 1 and 4 show the performance that is expected of this setup. Pump 2 has a higher maximum pressure head compared to pump 1 and 4, this is mainly due to differences in clamping force which holds the piezo's in place. An investigation was performed into the influence of the clamping force on the maximum pressure head which showed that a higher clamping pressure on the piezo elements is beneficial to the maximum pressure head. It can also be seen that pumps 3 and 5 underperform compared to what is expected. Additionally, pumps 3 and 5 perform differently when compared to each other. In both these pumps one piezo had stopped functioning, for pump 3 this was the first piezo and pump 5 the second piezo in series had stopped working. More invesetigation is needed into the reliability of the piezo's and the influence of assembly on the reliability.

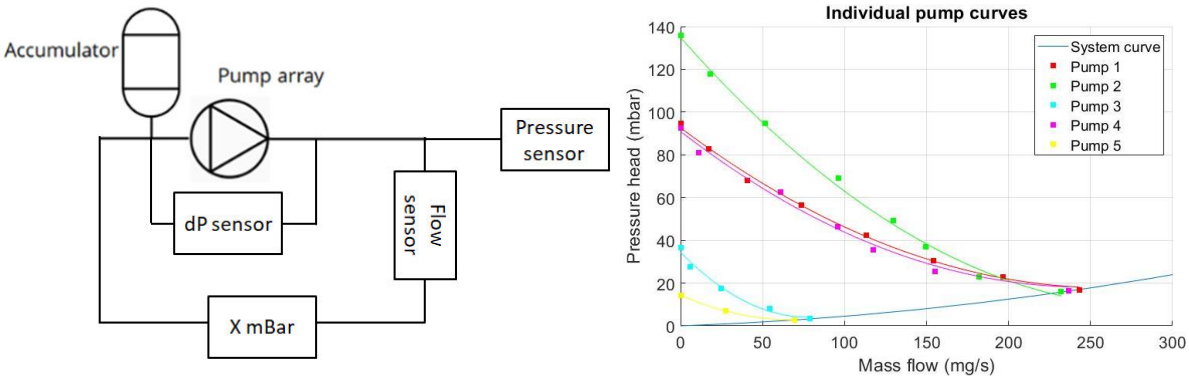

Figure 7: Left: schematic setup of individual pump testing with flow restriction indicated by "X mBar". Right: pump curves of individual micropumps in the overall pump, pumps are operated with 150V at 100Hz.

As a final step all multiple parallel micropumps were switched on to determine the overall pump curve. In this test all individual pump units in the pump housing are switched on and work in parallel. The total pump curve is shown in Figure 8 which includes the data points, the interpolation and expected extrapolation for lower system curve results. This pump curve includes the malfunctioning pumps 3 and 5, so better performance is expected for a future iteration of the pump.

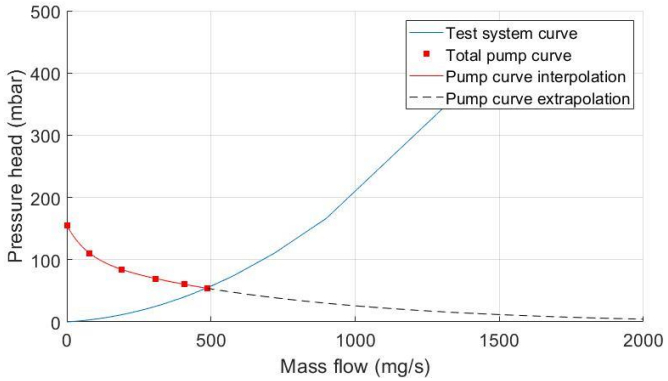

Figure 8: Pump curve of the total pump with all 5 individual pump units switched on. The measurement points are given in red squares. The extrapolation in based on expected results from individual pump units.

From Figure 8 it can be seen that the system curve is cutting of the interesting region of the pump curve; above 500 mg/s. The main cause for the steep system curve is the pressure drop in the pump housing, which has a detrimental effect on performance. Future iterations will aim to improve the design of the pump housing to further minimize the internal pressure drop. The maximum mass flow that was obtained during this test is 500 mg/s using Galden HT55 (18 mL/min). All tests were performed under multiple orientations and produced the same results. It is expected that an optimized pump can achieve 2 g/s of mass flow.

B. Accumulator testing

The accumulator was tested on its ability to apply pressure to the pumped loop. As it is not possible to directly measure the pressure inside the accumulator due to size limitations, the internal accumulator pressure was derived using the accumulator temperature and known T-P diagrams from the datasheet of Galden HT55. Figure 9 shows the pressure response of the loop and accumulator when the accumulator heater is switched on. It can be seen that the measured loop pressure lags behind the accumulator pressure. This is due to the fact that the loop pressure is measured outside of the accumulator and the elements in between cause a small pressure drop. The heater power used here is 8 Watts to demonstrate an extreme case. Typical operation requires up to 0.2 Watt of heater power when the accumulator is properly isolated using Multi-Layer Insulation (MLI) and mounting bolts with low thermal conductivity. The results show that the accumulator is indeed able to build up and control the pressure generated by the vapour phase of the

working fluid. The accumulator produced similar results when the orientation is changed, proving that the accumulator functions orientation independent.

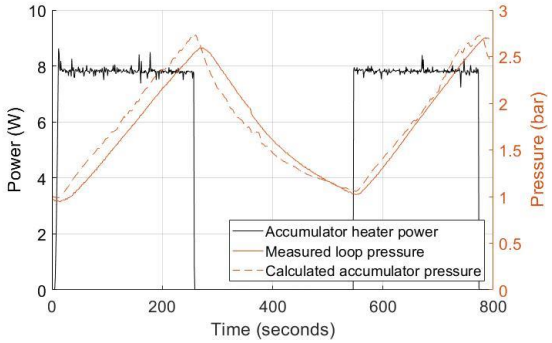

Figure 9: Measured loop pressure and calculated accumulator pressure (based on accumulator temperature) when the accumulator heater is switched on or off.

C. Integrated system testing

As a final test in the test-campaign, the pump with accumulator was integrated into a 2U CubeSat together with a demonstration payload and demonstration heat sink. Figure 10 shows the integrated pump and demonstration payload with heat exchanger. It can be seen that the pump and accumulator fit well within the CubeSat form factor. Its placement in the CubeSat is deliberately done on a location where normally no PCB plates would fit, so it only takes up unused volume. The dummy payload is a power resistor which can generate up to 20 Watt of heat. The entire setup is wrapped in insulating foam to minimize convective heat losses.

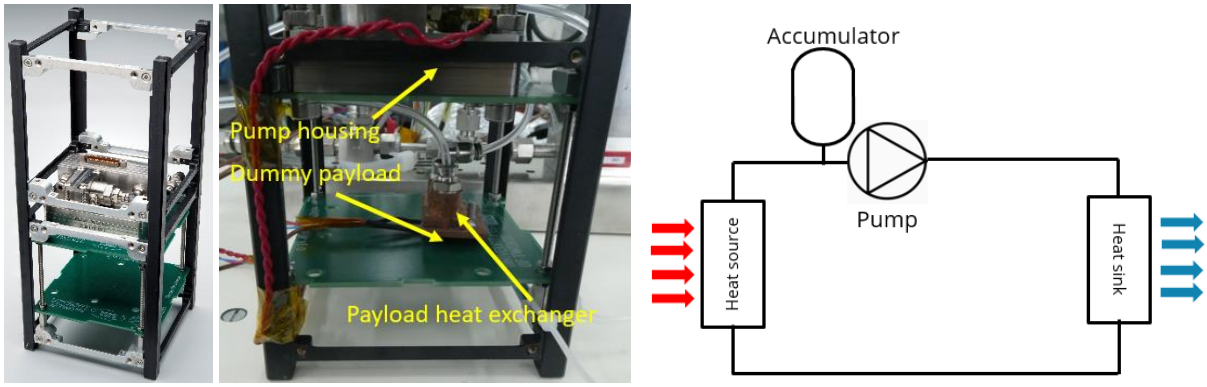

Figure 10: Pictures of the integrated pump housing with accumulator, setup of the dummy payload with heat exchanger and schematic overview of the integrated test setup.

The goal of the integrated system tests is to determine the temperature response of the payload and loop components when orbital temperatures of the heat sink are simulated. When a spacecraft enters eclipse, there is a rapid drop in temperature at the heat sink and a rapid rise when leaving eclipse. To mimic this effect, the temperature of the heat sink is externally controlled to follow a sunlight-eclipse-sunlight sinusoidal temperature. During this oscillation in temperature the temperature of the payload and loop components are monitored. Multiple cycles are then compared to see if every cycle is consistent. Additionally, it is also possible to determine the maximum payload power for which the cooling system functions independently of the specific (low-earth) orbit. Figure 11 shows the applied heat sink temperature and the response temperatures after the payload. The expected result determined by the model is also shown. A difference can be observed between the measured temperatures and the simulated transient result. This is due to residual convective heat losses and thermal capacity of the insulating foam, which is not taken into account in the simulation. Vacuum testing is required to further verify the transient model. Figure 12 shows the temperature difference over the payload heat exchanger as a function of input power, showing that the mini-MPL prototype can transport 20W of heat.

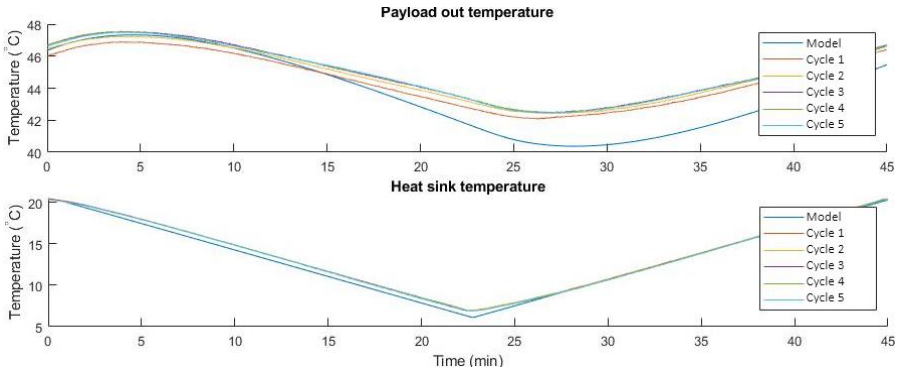

Figure 11: Payload out temperature response when the heat sink temperature is changed over time to mimic orbital eclipse-sunlight change under 10 Watt heat load.

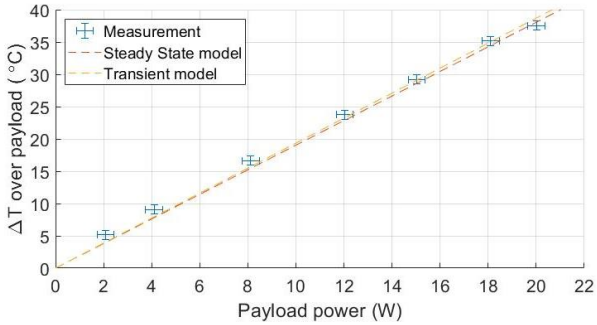

Figure 12: Demonstrated steady state heat transport capability of mini-MPL, mass flow of 500 mg/s.

VIII. Conclusion

A standardized thermal concept is proposed based on a two-phase mini-pumped loop. The system has a heat switch function and gives the possibility to cool P/L's with multiple hot spots such as electronics or small propulsion modules.

A mini MPL demonstrator has been constructed, using a multi-parallel prototype pump and integrated in a 2U CubeSat. A mass flow of 500 mg/s has been demonstrated as well as a steady state heat transport of 20 W and an orbit independent heat transport of 10 W. A model was created to predict the heat transport capability as well as transient temperature response of the mini MPL demonstrator. The model has demonstrated to be able to predict steady state heat transport of the mini MPL concept, however needs vacuum testing to be verified for transienst cases.

The multi-parallel micro pump concept uses a large set of micro-pumps which solves the single-point-of-failure drawback of ordinary micro-pumps. The system is extremely flexible and versatile to cover thermal control problems from 3U to 16U CubeSats. It is also applicable for series production for satellite swarms, especially for direct response missions for disaster monitoring or to support military reaction forces. The mini MPL concept is also viable for deep-space missions as it has an intrinsic heat switch functionality, preventing over-cooling of components. It is expected that future iterations of the multi-parallel micro pump have a total mass of 0.3 kg and can achieve a mass flow up to 2 g/s which allows the mini MPL to transport up to at least 80 W of heat.

References

1. H. Weeren, M. T. Brake, R. Hamann, G. Holl, and S. Price, "Thermal Aspects of Satellite Downscaling", Journal of Thermophysics and Heat Transfer 23, 592 (2009)
2. W. Hengeveld, M. R. Wilson, J. A. Moulton, B. S. Taft and A. M. Kwas, "Thermal Design Considerations for Future High-power Small Satellites," 48th International Conference on Environmental Systems, 2018
3. Personal communication with ESA, Philipp Hager (ESTEC, Thermal Control Section (TEC-MTT)
4. H.J. van Gerner., R. Bolder, J. van Es, "Transient modelling of pumped two-phase cooling systems: Comparison between experiment and simulation with R134a",47th Int. Conf. on Environmental Systems, Charleston, South Carolina, USA 2017
5. H.J. van Gerner, R.C. van Benthem, J. van Es, D. Schwaller, S. Lapensée," Fluid selection for space thermal control systems", 44th Int. Conf. on Environmental Systems, Tucson, Arizona USA, 2014